



Low-temperature thermal properties and features of the phonon spectrum of lutetium tetraboride



V.V. Novikov^a, N.V. Mitroshenkov^{a,*}, A.V. Matovnikov^a, D.V. Avdashchenko^a, A.V. Morozov^b, L.M. Pavlova^c, V.B. Koltsov^c

^aBryansk Petrovsky State University, 14 Bezhitskaya St., Bryansk 241037, Russia,

^bRussian Timiryazev State Agrarian University, 49 Timiryazevskaya St., Moscow 127550, Russia

^cNational Research University of Electronic Technology "MIET", Moscow 124498, Russia

ARTICLE INFO

Article history:

Received 7 May 2014

Received in revised form 5 June 2014

Accepted 5 June 2014

Available online 14 June 2014

Keywords:

Rare earth alloys and compounds

Heat capacity

Thermal expansion

Thermal analysis

ABSTRACT

The coefficients of thermal expansion to the *c* axis (α_{\parallel} , α_{\perp}) were measured for lutetium tetraboride over the temperature range 4.2–300 K. The heat capacity data for lutetium tetraboride were used for the calculation of tetraboride phonon spectrum moments and also for the development of a simplified tetraboride spectrum model. The use of the heat capacity and thermal expansion data allowed the temperature changes of the Grüneisen parameters Γ , Γ_{\parallel} , Γ_{\perp} for tetraboride to be calculated.

As a result of the approximation of $\Gamma_{\perp}(T)$, $\Gamma_{\parallel}(T)$ temperature dependencies in accordance with the chosen phonon spectrum model have been found: the anomalies of $\Gamma_{\perp}(T)$, $\Gamma_{\parallel}(T)$ are at about 25 K and then drop at lower temperatures due to the Einstein vibrations of boron sublattices.

© 2014 Published by Elsevier B.V.

1. Introduction

Tetraborides of rare-earth elements (RB₄ compounds, in which R stands for the rare-earth element), in addition to the high hardness and melting temperature typical of all rare-earth borides, also possess a number of properties making them rather interesting from the general scientific and practical perspectives. The application-oriented interest in rare-earth tetraborides is primarily conditioned by the magnetic and structural transformations occurring in most of them [1–10]. As a result of these transformations, a number of physical and thermodynamic characteristics change in discrete steps. Such changes in their properties can be used for producing various switching devices, magnetic cooling devices and so forth [11]. Of great theoretical interest is the research of the ordering processes in the tetraborides' magnetic sub-systems, which are, on the one hand, conditioned by the characteristic properties of R³⁺ paramagnetic ions and, on the other hand, by the peculiarity of their spatial location caused by the unique crystalline structure of RB₄ compounds.

Tetraborides of rare-earth elements are characterized by the tetragonal crystalline structure of the UB₄ type, $D_{2h}^5 - P4/mbm$. The unit cell contains four formula units [12].

Boron sub-lattice is made up of B₆ octahedra (the structural unit of the boron sub-lattice of rare-earth hexaborides), connected by chains of boron atoms, which, together with the octahedron ribs, form the distorted heptangular rings. This ring-shaped arrangement of boron atoms is characteristic of rare-earth diborides. A tetraboride lattice is represented as alternate layers of metal and boron atoms (Fig. 1) [13].

Above the rings of boron atoms there are metal atoms which form squares and triangles in the plane perpendicular to the crystal *c* axis. This mutual arrangement of R³⁺ paramagnetic ions corresponds to the so-called Shastry–Sutherland lattice (SSL), the most characteristic feature of which is a geometric frustration, that is the impossibility of complete ordering in the system of atomic magnetic moments up to the absolute zero [14] and, as a consequence, the presence of zero-point entropy [15–17].

For the successful study of the features of electronic and magnetic sub-systems of the magnetic materials, it is often necessary to single out the influence of the phonon sub-system on the values of the properties under study. To evaluate the lattice contribution to the characteristics of magnetic materials, the method of comparison with the non-magnetic isostructural analogue is usually employed. For the family of rare-earth tetraborides these diamagnetic analogues are lanthanum and lutetium tetraborides (LaB₄ and LuB₄ respectively).

As follows from the phase diagrams and our experiments, it is much more difficult to synthesize the single-phased sample of

* Corresponding author.

E-mail addresses: vvnovikov@mail.ru (V.V. Novikov), weerm@yandex.ru (N.V. Mitroshenkov).

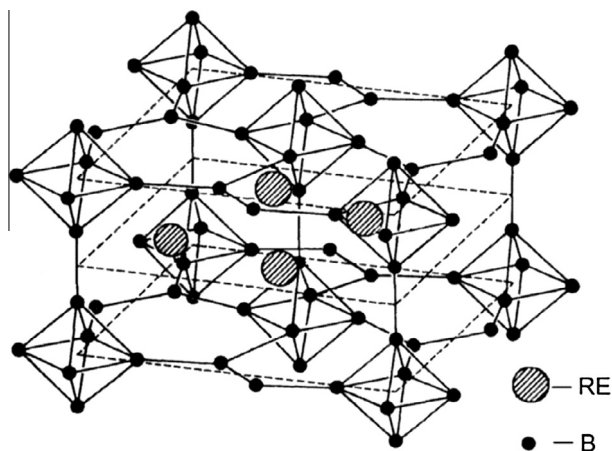
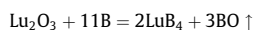


Fig. 1. The unit cell of RB_4 .

lanthanum tetraboride than lutetium tetraboride. Therefore, to study the phonon properties of rare-earth tetraborides at low temperatures, the lutetium tetraboride was chosen (LuB_4).

2. Experiment

The polycrystalline sample of lutetium tetraboride was synthesized by the method of boron-thermal reduction of metal from its oxide in a vacuum [17]:



For the synthesis we used lutetium oxide of 99.9% purity produced by Mosreaktiv, as well as the elemental boron of 99% purity produced by ErmakKhim. The synthesis was carried out in the vacuum electric furnace manufactured by Termotekhnik ML. At the first stage of synthesis, we annealed the stoichiometric mixture of oxide and boron at a temperature of $T_1 = 1473$ K for 3 h at a pressure of 10^{-1} Pa. The X-ray diffraction pattern of the synthesized sample obtained by the X-ray diffractometer DRON-7 (Burevestnik Research and Manufacturing Association) in $Co K\alpha$ radiation was compared to the ASTM data and contained the reflections of tetraboride, oxide and metal phases (Fig. 2a). To eliminate the excess phases, the sample, previously comminuted to a powdery condition and then compacted into a tablet, underwent additional annealing at a temperature of $T_1 = 1973$ K for 1 h. After the second annealing, the X-ray diffraction pattern contained the reflexes of the only phase – the LuB_4 phase (Fig. 2b). According to the chemical analysis, the synthesized sample contains 19.74% lutetium, and 80.27% boron. The crystalline lattice parameters for the LuB_4 sample were as follows: $a = 0.70336$ nm, $c = 0.39732$ nm (according to [12] $a = 0.7036$ nm, $c = 0.3974$ nm).

The a and c lattice parameters for lutetium tetraboride in the temperature range of 5–300 K were determined by the Debye–Scherrer method using the X-ray diffractometer DRON-7.0 in $Co K\alpha$ radiation with Bragg–Bretanno focusing. From the synthesized LuB_4 powder, a tablet 13 mm in diameter and 1 mm thick was formed by means of pressing with a small amount of an organic binding agent. The tablet was placed in the copper cuvette of the X-ray helium cryostat, which was equipped with a constantan wire heater 0.05 mm thick. The signal from the ‘Constantan–Copper +0.1% Iron’ thermocouple, whose junction point was adjusted to the copper

cuvette, reached the temperature regulator which kept the cuvette temperature in the range of 5–300 K with an accuracy of not less than 0.05 K. To find the values for the a and c lattice parameters of lutetium tetraboride we experimentally worked out the angle positions for θ Bragg reflections (214) and (271) at room temperature: $2\theta_{214} = 141.6^\circ$ and $2\theta_{271} = 144.6^\circ$. These reflections belong to the high-angle region of scattering and are well-represented. At room temperature, the Bragg angles of scattering for 28 reflexes were evaluated. Then the $a_{hkl}(\cos^2 \theta_{hkl})$, $c_{hkl}(\cos^2 \theta_{hkl})$ dependencies were calculated, which were extrapolated to zero. The ordinate intersection of $a_{tr}(300 K) = 0.70336$ nm, $c_{tr}(300 K) = 0.39732$ nm were considered the true values of the a and c parameters for lutetium tetraboride at room temperature. Differences $\Delta a = a_{tr}(300 K) - a_{\theta_1, \theta_2}(300 K)$, $\Delta c = c_{tr}(300 K) - c_{\theta_1, \theta_2}(300 K)$ were considered as constant values within the whole temperature range and were used as corrections to the values of $a_{\theta_1, \theta_2}(T)$, $c_{\theta_1, \theta_2}(T)$. Here θ_1, θ_2 are the reflex scattering angles (214) and (271), respectively, within the range of 4.2–300 K.

The heat capacity of the LuB_4 sample in the range of 2–300 K was measured in the adiabatic vacuum calorimeter produced by Termax, the construction of which is similar to the one described above [18]. The sample temperature in the process of the calorimetric experiment was measured using a ferrous-rhodium thermometer with an accuracy of ± 0.05 K. The experimental adiabatic conditions were automatically maintained. In each heating cycle, the sample temperature increased by 0.2–0.5 K. The inaccuracy of the heat capacity evaluation amounted to 3% at 2–20 K. At 60 K it decreased to 1% and remained within this range up to the room temperatures. The difference in the calibration measurement results of the sample of electrolytic copper, annealed and melted in the vacuum, from the recommended values [19] did not exceed the inaccuracy indicated above.

3. Results and discussion

In Table 1, one can see the smoothed values of $C_p(T)$ LuB_4 molar heat capacity in the temperature range under study. Fig. 2a and b illustrate the experimental dependencies of $C_p(T)$, $C_p/T^3(T^2)$. $C_p(T)$ dependency (Fig. 2a) has the features typical of diamagnetic rare-earth borides within the range of low temperatures [20]. One can clearly see the smooth anomaly of the $C_p(T)$ curve within the range of 25–75 K and the dependency close to the linear at the higher temperatures (100–300 K). The bell-shaped maximum at the dependency $C_p/T^3(T^2)$ (Fig. 2b) signals the presence of Einstein components for LuB_4 heat capacity. The increase in the $C_p/T^3(T^2)$ curve is conditioned by the contribution of the electron gas into the boride heat capacity: $C_{el} = 0.00017$ J/g at K.

We approximated the phonon spectrum of lutetium tetraboride by the following expression:

$$G(\omega) = a_1\omega^3 + a_2\omega^3 + a_3\delta(\omega - \omega_{1E}) + a_4\delta(\omega - \omega_{2E}),$$

$$\omega < \omega_{1\max} \quad \omega < \omega_{2\max} \quad (1)$$

where a_1, a_2 are determined from the values of the characteristic Debye temperatures of θ_{1D}, θ_{2D} ; and ω_{1m}, ω_{2m} are frequencies at which Debye parabolic phonon spectra are cropped. The values of these spectra as well as the a_3, a_4 coefficients, were chosen for the best correspondence to the experimental data.

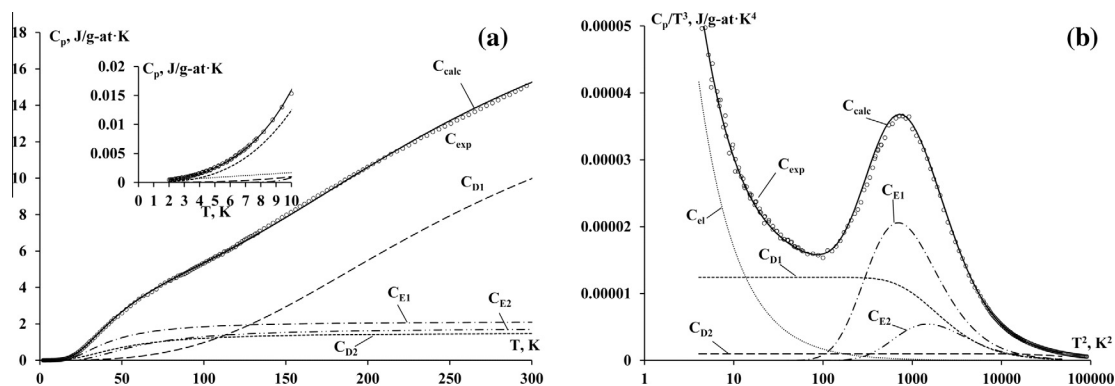


Fig. 2. Lutetium tetraboride heat capacity (a) $C_p(T)$ dependency and (b) $C_p/T^3(T^2)$ dependency.

Table 1
Lattice parameters a (nm), c (nm) and heat capacity C_p (J/mol K) of LuB₄.

T, K	a	c	C_p	T, K	a	c	C_p
2	–	–	0.0023	100	0.70282	0.39687	26.7758
4	0.70275	0.39680	0.0078	110	0.70284	0.39689	29.1590
6	0.70275	0.39680	0.0190	120	0.70286	0.39691	31.3624
8	0.70275	0.39680	0.0390	140	0.70290	0.39694	37.0540
10	0.70274	0.39680	0.0767	160	0.70294	0.39699	42.6100
20	0.70274	0.39679	1.1740	180	0.70299	0.39703	47.7670
30	0.70274	0.39680	4.6068	200	0.70304	0.39708	53.1099
40	0.70275	0.39680	8.8911	220	0.70310	0.39712	57.8709
50	0.70276	0.39681	12.6719	240	0.70316	0.39717	62.7623
60	0.70277	0.39682	16.4428	260	0.70322	0.39722	67.0953
70	0.70278	0.39683	19.2591	280	0.70329	0.39727	71.5559
80	0.70279	0.39684	21.9727	300	0.70336	0.39732	76.1250
90	0.70281	0.39686	24.2005				

The resulting heat capacity of LuB₄ in the given approximation is represented as the sum of Debye and Einstein components and the electron gas contribution:

$$C = a_1 C_D \left(\frac{T}{\theta_{D1}} \right) + a_2 C_D \left(\frac{T}{\theta_{D2}} \right) + a_3 C_E \left(\frac{T}{\theta_{E1}} \right) + a_4 C_E \left(\frac{T}{\theta_{E2}} \right) + a_5 T \quad (2)$$

The satisfactory approximation of the $C_p(T)$ experimental dependency for lutetium tetraboride was achieved with the following parameter values: $\theta_{D1} = 1140$ K, $\theta_{D2} = 211$ K, $\theta_{E1} = 130$ K, $\theta_{E2} = 190$ K, $a_1 = 0.7$, $a_2 = 0.06$, $a_3 = 0.085$, $a_4 = 0.07$, $a_5 = 0.00017$ J g at.⁻¹ K⁻².

The highly informative characteristics of the crystal phonon sub-system are the moments of its phonon spectrum [21]:

$$\mu_n \frac{1}{6N} \int_0^\infty v^n G(v) dv$$

$$\mu_n^* = \left(\frac{h}{k} \right)^n \mu_n,$$

where N is the Avogadro constant, v is frequency, $G(v)$ is the frequency distribution function (phonon spectrum), h is the Planck constant and k is the Boltzmann constant. To compare the moments of different order it is customary to use the moment function $v_D(n)$:

$$v_D(n) = \left\{ \frac{1}{3}(n+3)\mu_n \right\}^{\frac{1}{n}}$$

In the Debye approximation $v_D(n) = \text{const}$.

The μ_i value for the lutetium tetraboride was similarly calculated [22].

The resulting calculations of the phonon spectrum moments of lutetium tetraboride are represented in Table 2.

The value of μ_2 determines the limit value of the characteristic temperature at infinity: $\theta^\infty = \frac{h}{k} \left(\frac{2\mu_2}{3} \right)^{\frac{1}{2}} = 1081$ K.

The temperature changes of LuB₄ $S(T)$ entropy make it possible to determine the value of $v_D(0)$, and consequently the mean frequency of the phonon spectrum: $e^{\frac{1}{2}} h v_q = h v_D(0)$ [21]. For LuB₄ $v_q = 1.22 \times 10^{13}$ c⁻¹.

The energy of the lattice zero-point oscillations (E_Z) is determined from the moment μ_1 : $v_q = 1.22 \times 10^{13}$ c⁻¹.

$v_D(n)$ dependency is represented in Fig. 3.

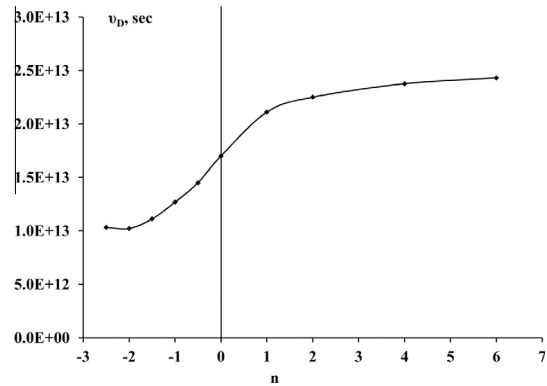


Fig. 3. $v_D(n)$ dependency on moment number for LuB₄ phonon spectrum.

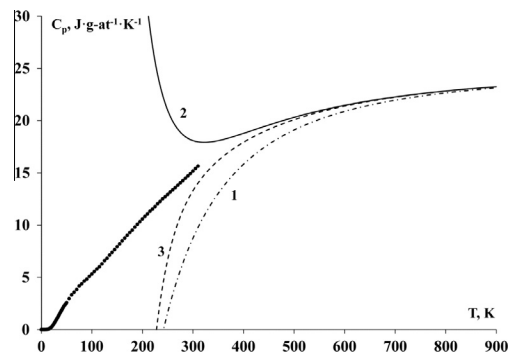


Fig. 4. LuB₄ heat capacity approximations at high temperatures by the moments of phonon spectrum (points – experimental data, 1 – one moment, 2 – two moments, 3 – three moments).

Fig. 4 shows LuB₄ dependency curves $C_p(T)$ within the high temperature range calculated by the Thirring method [23] using the obtained moments as compared to the experimental low-temperature data. As can be seen from the figure, the use of moments of higher order makes it possible to better approximate to the experimental data.

4. Thermal expansion

The experimental values of a and c lattice parameters for LuB₄, obtained in the present research, are represented in Fig. 5. The smoothed values of $a(T)$ and $c(T)$, smoothed by least squares method, are represented in Table 1.

Within the biggest part of the temperature range under study on $a(T)$ and $c(T)$ dependencies, there are no explicit anomalies. Close to the absolute zero – at about 20 K – both $a(T)$ and $c(T)$ dependencies have their minimum. In the area lower than 10 K the temperature decrease is accompanied by lattice expansion. This anomalous behaviour of the crystalline structure can be conditioned by different reasons. In particular, the negative expansion at the lowest temperatures can be caused, for instance, by the influence of the conduction electrons, as well as by the peculiarities of the crystalline lattice sub-system [24]. The revealed anomalies are more distinct on the temperature dependencies of the coefficients of linear α_a , α_c and volume β thermal expansion (Fig. 6).

Table 2
The phonon spectrum moments of lutetium tetraboride.

$\mu(-2, 5), s^{-2.5}$	$\mu(-2), s^{-2}$	$\mu(-1, 5), s^{-1.5}$	$\mu(-1), s^{-2.5}$	$\mu(-0.5), s^{-2.5}$	$\mu(1), s$	$\mu(2), s^2$	$\mu(4), s^4$	$\mu(6), s^6$
1.76×10^{-32}	2.87×10^{-26}	5.4×10^{-20}	1.18×10^{-13}	3.15×10^{-7}	1.58×10^{13}	3.04×10^{-26}	1.37×10^{53}	6.88×10^{79}

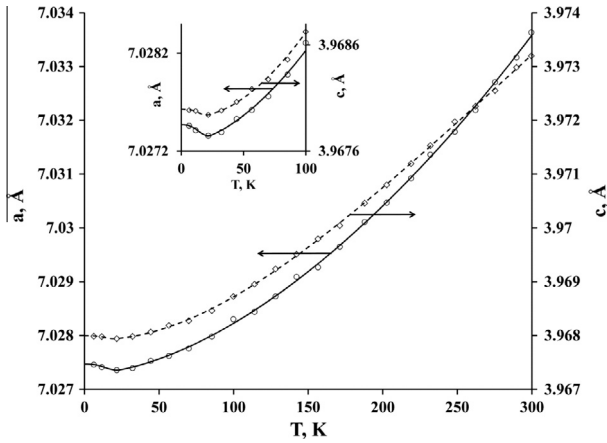


Fig. 5. $a(T)$, $c(T)$ lattice parameters for lutetium tetraboride at 5–300 K. Open circle – the experimental data, the solid curves – the smoothed dependencies.

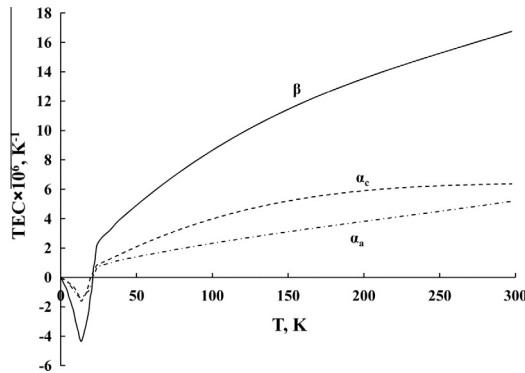


Fig. 6. Temperature dependency of LuB_4 linear thermal expansion coefficient: dash-and-dot line – $\alpha_a(T)$; dotted line – $\alpha_c(T)$; solid line – $\beta(T)$.

The revealed peculiarities of LuB_4 thermal expansion were analysed on the basis of calculating the temperature dependencies of the boride Grüneisen parameter, $\Gamma = \frac{\beta V}{\gamma C_V}$ where β is the volume expansion coefficient; C_V is isochoric molar heat capacity, the value of which, in the first approximation, we considered to be equal to the isobaric heat capacity C_p . In the quasi-harmonic approximation, the γ value represents the weight-average of the i -th mode Γ_i of the phonon spectrum, where the weight coefficients of each mode are the contributions of those modes to the heat capacity [25]:

$$\gamma = \frac{\sum_i^m C_i \gamma_i \Gamma_i}{\sum_i^m \Gamma_i} \quad (3)$$

Two Grüneisen functions Γ_{\perp} , Γ_{\parallel} correspond to the $\alpha_a(T)$, $\alpha_c(T)$ linear thermal expansion coefficients. For the tetragonal structure they are determined as follows [25]:

$$\gamma_{\perp}(T) = \frac{V}{C_p} (C_{11} + C_{11})\alpha_a + C_{13}\alpha_c \quad (4)$$

$$\gamma_{\parallel}(T) = \frac{V}{C_p} C_{13}\alpha_a + C_{33}\alpha_c \quad (5)$$

Here, c_{xy} are the adiabatic elastic constants and $C_p(T)$ is the heat capacity at the constant volume.

The values of Γ_{\perp} , Γ_{\parallel} calculated according to the data on LuB_4 thermal expansion and elastic constants from [26] (Eqs. (4), (5)) are represented in Fig. 7. As one can see from the figure, the values of Γ_{\perp} , Γ_{\parallel} within the whole temperature range under study are close to each other.

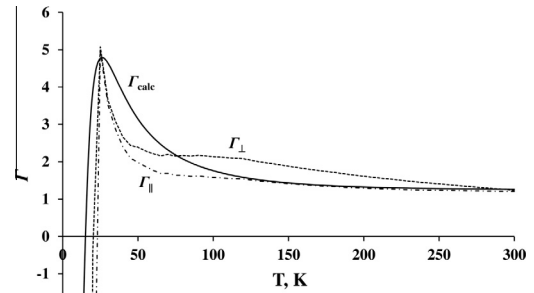


Fig. 7. Grüneisen parameters for lutetium tetraboride.

The peculiarities of $\Gamma_{\perp}(T)$, $\Gamma_{\parallel}(T)$ dependencies are: (1) the distinct maximum at about 25 K; (2) the steep downfall with the transition to the negative area at the further temperature decrease.

To understand which factors influence this behaviour of the $\Gamma_{\perp}(T)$, $\Gamma_{\parallel}(T)$ dependencies, we calculated these values using Eq. (3), which, according to approximation (1), is as follows:

$$\Gamma_{\parallel} = \frac{k_1 C_{D1} \Gamma_{\parallel 1} + k_2 C_{D2} \Gamma_{\parallel 2} + k_3 C_{E1} \Gamma_{\parallel 3} + k_4 C_{E2} \Gamma_{\parallel 4}}{k_1 C_{D1} + k_2 C_{D2} + k_3 C_{E1} + k_4 C_{E2}} \quad (6)$$

$$\Gamma_{\perp} = \frac{k_1 C_{D1} \Gamma_{\perp 1} + k_2 C_{D2} \Gamma_{\perp 2} + k_3 C_{E1} \Gamma_{\perp 3} + k_4 C_{E2} \Gamma_{\perp 4}}{k_1 C_{D1} + k_2 C_{D2} + k_3 C_{E1} + k_4 C_{E2}} \quad (7)$$

Here k_i are the coefficients of i -th mode contributions to heat capacity (Eq. (2)); and C_{Di} , C_{Ei} are Debye and Einstein functions of heat capacity. Since $\Gamma_{\perp} \approx \Gamma_{\parallel}(T)$ within the whole temperature range, we used one of the equations, Eq. (7) for the selection of the values Γ_{calc} . The best correspondence to the experimental $\Gamma_{\perp}(T)$, $\Gamma_{\parallel}(T)$ dependencies was achieved at the following Γ_i values: $\Gamma_1 = -10$; $\Gamma_2 = 1.2$; $\Gamma_3 = 14.9$; $\Gamma_4 = -5.5$.

The dependency calculated according to Eq. (6) is represented in Fig. 7. While selecting Γ_{\perp} , Γ_{\parallel} values, it was revealed that the experimental peculiarities of $\Gamma_{ji}(T)$ dependencies, that is, the distinct maximum around 20 K and the steep downfall at the further temperature lowering, are shaped by varying the Γ_{i3} , Γ_{i4} values, that is, these peculiarities observed in the area of negative expansion are conditioned by the Einstein oscillations of the boron sub-lattice.

We made an attempt to eliminate the steep downfall of $\Gamma_i(T)$ dependencies at the lowest temperatures by means of considering the electron contribution to LuB_4 thermal expansion (Eq. (35) from [27]). However, even at very large values of the electron Grüneisen parameter (in which Γ_e amounts to 100 units and more) we failed to find any significant influence of the electron contribution on $\Gamma_i(T)$ dependency.

5. Conclusions

The complex calorimetric and X-ray research of the properties of lutetium tetraboride conducted for the first time enabled us to define the type of the LuB_4 phonon spectrum within the accepted Debye–Einstein model, as well as to single out the anomalies of the boride thermal characteristics and to ascertain the cause of these anomalies.

The values of the phonon spectrum moments determined from the $C_p(T)$ temperature dependency made it possible to single out the important characteristics of LuB_4 phonon sub-systems which are the characteristic temperatures at absolute zero and at infinity, the mid-geometric frequency of the phonon spectrum, and the lattice zero-oscillation energy.

As a result of the conducted analysis of the experimentally obtained peculiarities of the temperature dependencies of LuB_4 heat capacity and heat expansion it was found that:

- (1) the temperature dependency $C_p(T)$ of the LuB_4 heat capacity within the range of 2–300 K can be satisfactorily approximated by the sum of two Debye and two Einstein components, taking into account the electron contribution to the heat capacity; the conducted analysis enabled us to evaluate the characteristic temperatures and the parts of the described contributions to the boride complete heat capacity; on the basis of the obtained data we offered the model of the LuB_4 phonon spectrum, which is represented as the sum of contributions of two Debye parabolas and two Einstein δ -functions;
- (2) the negative thermal expansion of lutetium tetraboride at temperatures lower than 20 K has a lattice nature and is conditioned by the Einstein oscillation of the boron sub-lattice.

Acknowledgements

The research was undertaken under the auspices of The Ministry of Education and Science of the Russian Federation (State Assignment No. 2014/426 for 2014–2016) and the Russian Foundation for Basic Research (Grant No. 14-02-31692 mol_a).

References

- [1] D. Okuyama, T. Matsumura, H. Nakao, Y. Murakami, Quadrupolar frustration in Shastry-Sutherland lattice of DyB_4 studied by resonant X-ray scattering, *J. Phys. Soc. Jpn.* 74 (2005) 2434–2437.
- [2] Z. Fisk, M.B. Maple, D.C. Johnston, L.D. Woolf, Multiple phase transitions in rare earth tetraborides at low temperature, *Solid State Commun.* 39 (1981) 1189–1192.
- [3] B.K. Cho, J.-S. Rhyee, J.Y. Kim, M. Emilia, P.C. Canfield, Anomalous magnetoresistance at low temperatures ($T < 10$ K) in a single crystal of GdB_4 , *J. Appl. Phys.* 97 (2005) 10A923.
- [4] G. Oomi, M. Ohashi, B. Cho, Effect of pressure on the anomalous magnetoresistance and antiferromagnetism of single crystal GdB_4 , *J. Phys: Conf. Ser.* 176 (2009) 012038.
- [5] K.H.J. Buschow, J.H.N. Creighton, Magnetic properties of rare earth tetraborides, *J. Chem. Phys.* 57 (1972) 3910.
- [6] A. Berrada, J.P. Mercurio, B. Chevalier, J. Etourneau, P. Hagenmuller, M. Lalanne, J.C. Gianduzzo, R. Georges, Synthèse, cristallogenèse, propriétés magnétiques et effets magnétostrictifs spontanés de quelques tetraborures de terres rares, *Mater. Res. Bull.* 11 (1976) 1519–1526.
- [7] R. Watanuki, G. Sato, K. Suzuki, M. Ishihara, T. Yanagisawa, Y. Nemoto, T. Goto, Geometrical quadrupolar frustration in DyB_4 , *J. Phys. Soc. Jpn.* 74 (2005) 2169–2172.
- [8] T. Matsumura, D. Okuyama, Y. Murakami, Non-collinear magnetic structure of TbB_4 , *J. Phys. Soc. Jpn.* 76 (2006) 015001.
- [9] T. Suzuki, T. Fujita, I. Ishii, S. Michimura, F. Iga, T. Takabatake, Large softening of longitudinal elastic modulus in TbB_4 , *J. Phys: Conf. Ser.* 150 (2009) 042194.
- [10] S. Mat'áš, K. Siemensmeyer, E. Wheeler, E. Wulf, R. Beyer, T. Hermannsdörfer, et al., Magnetism of rare earth tetraborides, *J. Phys: Conf. Ser.* 200 (2010) 032041.
- [11] Z. Han, D. Li, H. Meng, X.H. Liu, Z.D. Zhang, Magnetocaloric effect in terbium diboride, *J. Alloy. Comp.* 498 (2010) 118–120.
- [12] Z.P. Yin, W.E. Pickett, Rare-earth-boron bonding and 4f-state trends in RB_4 tetraborides, *Phys. Rev. B* 77 (2008) 35135.
- [13] W. Schäfer, G. Will, The crystal structures of ErB_4 and DyB_4 studied by neutron diffraction, *Z. Kristallogr.* 144 (1976) 217–225.
- [14] B.S. Shastry, B. Sutherland, Exact ground state of a quantum mechanical antiferromagnet, *Physica* 108B (1981) 1069–1070.
- [15] V.V. Novikov, A.V. Matovnikov, N.V. Mitroshenkov, A.V. Morozov, D.V. Avdashchenko, Thermal properties of TbB_4 , *J. Therm. Anal. Calorim.* 113 (2013) 779–785.
- [16] V.V. Novikov, N.V. Mitroshenkov, A.V. Morozov, A.V. Matovnikov, D.V. Avdashchenko, Heat capacity and thermal expansion of gadolinium tetraboride at low temperatures, *J. Appl. Phys.* 111 (2012) 063907.
- [17] V.V. Novikov, A.V. Morozov, A.V. Matovnikov, D.V. Avdashchenko, Y.N. Polesskaya, N.V. Sahoshko, B.I. Kornev, V.D. Solomennik, V.V. Novikova, Low-temperature heat capacity of RE-tetraborides, *Phys. Solid State* 53 (2011) 1839–1844.
- [18] N.N. Sirota, V.V. Novikov, A.M. Antjukhov, Thermodynamic properties of gallium arsenide and indium arsenide solid solutions in the temperature range of 5–300 K, *Russ. J. Phys. Chem.* 57 (1983) 542–547.
- [19] N.P. Rybkin, N.G. Nurullaev, A.K. Baranjuk, Z.P. Leskova, The using of copper as exemplary substance in low-temperature calorimetry, *Trudy VNIIFTRI (Russ.)* 4 (1972) 244–256.
- [20] V.V. Novikov, Components of the low-temperature heat capacity of rare-earth hexaborides, *Phys. Solid State* 43 (2001) 300–304.
- [21] E.W. Montroll, Frequency spectrum of crystalline solids, *J. Chem. Phys.* 10 (1942) 218.
- [22] V.V. Novikov, A.V. Matovnikov, D.V. Avdashchenko, B.I. Kornev, V.D. Solomennik, V.V. Novikova, O.A. Marakhina, Specific features of phonon subsystems in diborides of rare-earth element, *Phys. Solid State* 1–5 (2010) 142–147.
- [23] P. Flubacher, A.J. Leadbetter, J.A. Morrison, The heat capacity of pure silicon and germanium and properties of their vibrational frequency spectra, *Philos. Mag.* 39 (4) (1959) 273–294.
- [24] S.I. Novikova, Thermal Expansion of Solids, *Nayka*, Moscow, 1974.
- [25] M. Hortal, A.J. Leadbetter, The low temperature thermal expansion and Grüneisen function of tellurium, *J. Phys. C: Solid State Phys.* 5 (1972) 2129–2137.
- [26] E. Deligoz, H. Ozisik, K. Colakoglu, G. Surucu, Y.O. Ciftci, Mechanical and phonon properties of the superhard LuB_2 , LuB_4 , and LuB_{12} compounds, *J. Alloys Comp.* 509 (2011) 1711–1715, <http://dx.doi.org/10.1016/j.jallcom.2010.10.015>.
- [27] T.H.K. Barron, R.W. Munn, Analysis of the thermal expansion of anisotropic solids: application to zinc, *Philos. Mag.* 15 (1967) 85–103.